The influence of nitric acid on the cloud processing of aerosol particles

S. Romakkaniemi, H. Kokkola, K. E. J. Lehtinen, A. Laaksonen

Atmos. Chem. Phys. Discuss., 5, 10197–10216, 2005
www.atmos-chem-phys.org/acpd/5/10197/
SRef-ID: 1680-7375/acpd/2005-5-10197
European Geosciences Union

Atmospheric Chemistry and Physics Discussions

The influence of nitric acid on the cloud processing of aerosol particles

S. Romakkaniemi[1], H. Kokkola[1], K. E. J. Lehtinen[2], and A. Laaksonen[1]

[1]Department of Applied Physics, University of Kuopio, P.O. BOX 1627, FIN-70211 Kuopio, Finland
[2]University of Kuopio and Finnish Meteorological Institute, Department of Applied Physics, P.O. BOX 1627, FIN-70211 Kuopio, Finland

Received: 14 September 2005 – Accepted: 30 September 2005 – Published: 20 October 2005

Correspondence to: S. Romakkaniemi (sami.romakkaniemi@uku.fi)

Abstract

In this paper we present simulations of the effect of nitric acid (HNO_3) on cloud processing of aerosol particles. Sulfuric acid (H_2SO_4) production and incloud coagulation are both affected by condensed nitric acid as nitric acid increases the number of cloud droplets, which will lead to smaller mean size and higher total surface area of droplets. Increased acidity due to HNO_3 affects the H_2SO_4 production. As a result of increased cloud droplet number concentration (CDNC), the incloud coagulation rate is enhanced, so that the number of interstitial particles reduces faster. In addition, sulfuric acid production occurs in smaller particles and this will lead to higher number of particles in the accumulation mode.

1. Introduction

Cloud processing, both physical and chemical, is known to efficiently shape aerosol particle size distributions (Hoppel et al., 1994). Cloud droplets grow by condensation of different gases and by coagulation with other cloud droplets and interstitial particles. Volatility of condensed substances may change due to liquid phase chemistry. For example the oxidation of sulfur dioxide (SO_2) produces H_2SO_4 and the hydrolysis of N_2O_5 produces HNO_3 (see e.g. Seinfeld and Pandis, 1998). Most of sulfuric acid and some of nitric acid (depending on the conditions, for example the amount of ammonia present) will stay in the particles also when cloud droplets evaporate. Hence the dry particle size distribution and the chemical composition are altered by chemical processes. This will change the radiative properties of the aerosols (Yuskiewicz et al., 1999; Hegg et al., 2004) and it also affects the number of cloud condensation nuclei (CCN) (Bower and Choularton, 1993; Feingold and Kreidenweis, 2000). Coagulation decreases the number concentration of both interstitial particles and cloud droplets. The mean size of cloud droplets increases and some of the cloud droplets grow big enough to form precipitation. Coagulation processes are also important in nonprecipi-

ACPD

5, 10197–10216, 2005

tating clouds. Nucleation mode particles coagulate rapidly with cloud droplets and also the number of Aitken mode particles decreases rapidly compared to cloud free conditions. As a consequence, the radiative properties of aerosols as well as the properties of clouds during the next cloud cycle are modified.

Previous cloud model studies have shown that trace gases like HNO_3 and ammonia (NH_3) can increase cloud droplet number concentrations significantly (Kulmala et al., 1993; Hegg, 2000; Romakkaniemi et al., 2005; Xue and Feingold, 2004). This will reduce the mean cloud droplet size and thus increase cloud albedo and reduce precipitation efficiency, which increases cloud lifetime. Overall this will lead to a cooling of the lower troposphere and thus the effect is opposite in sign to the warming effect of greenhouse gases. Previously, the effect of HNO_3 on precipitation formation has been studied by Roelofs and Jongen (2004). They found that at low updraft velocities rain formation is delayed. Xue and Feingold (2004) found that the condensation of HNO_3 broadens the cloud droplet distribution and this should also be taken into account when estimating cloud optical properties.

HNO_3 affects also the cloud processing of aerosol particles. Increased droplet number and decreased size change the rate of droplet-droplet collisions and also the coagulation rate between droplets and interstitial particles changes. Furthermore, the H_2SO_4 production occurring in clouds is modified, as HNO_3 induces a higher droplet concentration so that number of particles in the accumulation mode present after cloud evaporation increases. As a consequence of coagulation and liquid phase chemistry, the cloud droplet number concentration and cloud properties are modified during the forthcoming cloud cycles. Also the radiative properties of aerosol particles can be changed.

In this study we present cloud model results on the effects of nitric acid on the formation of sulfuric acid and incloud scavenging of aerosol particles. We use a highly accurate air parcel model including differential equations for relevant physical and chemical processes. Due to the limitation of the modelling framework, we can not model the gravitational settling of drizzle limiting the study to nonprecipitating clouds.

2. Model

We apply an air parcel model with a moving sectional representation of the evolution of the aerosol size distribution to simulate the CCN activation to cloud droplets and dynamics of interstitial particles and cloud droplets in adiabatic cloud parcels. Included in the model are differential equations describing condensation, evaporation, coagulation, chemical reactions in the liquid and gas phases, adiabatic variables and the emissions of gas phase species. The model, excluding the coagulation module, has been described elsewhere (Kokkola, 2003), and so the model is described here only shortly. The differential equations are solved using ode-solver DLSODE [www.netlib.org], which solves initial-value problems for stiff or non-stiff ordinary differential equations using backward differentiation formulae.

The liquid phase thermodynamics and initial equilibration are calculated with a modified version of EQUISOLV II, which is a chemical equilibrium code developed by Jacobson (1999). The original EQUISOLV II uses the Zdanovskii-Stokes-Robinson (ZSR) method to estimate the liquid water content. This method is not very good for dilute solutions. For our purpose, it is changed so that the water activity is calculated with the method presented by Bromley (1973). The original and modified versions of EQUISOLV II showed a good consistency at RH's between 90 and 98% (Kokkola et al., 2003).

The coagulation kernel consists of five different parts: Brownian coagulation K_B, gravitational collection K_G, convective Brownian diffusion enhancement K_{BE}, turbulent inertia K_{TI}, and turbulent shear K_{TS}. The first one is caused by random movement of particles in the carrier gas. The second one is caused by different gravitational settling velocities. The third one, caused by eddies forming behind the large particles falling in the gas, is not as well established (Pruppacher and Klett, 1997). These eddies enhance the diffusion of smaller particles onto the surface of falling particle. The fourth and the fifth kernels are caused by turbulence in the air, which will lead to collisions due to inability of particles to follow the eddies due to their inertia and due to the

ACPD
5, 10197–10216, 2005

different velocities between particles because of turbulent shear. In this study we use expressions for the individual coagulation kernels as e.g. in Jacobson (1999) and estimate the total coagulation kernel as (Saffman and Turner, 1956)

$$K_{tot} = K_B + K_{BE} + \left(K_G^2 + K_{TI}^2 + K_{TS}^2\right)^{1/2}. \quad (1)$$

During coagulation, the mass of the coagulating particles is moved to the size class corresponding to the size of formed particle. It is assumed that the particles are internally mixed and the mixing within a size class occurs instantaneously after the coagulation. Because of the moving sections, the size class in which the formed particle is placed, is determined during the simulation continuously. In the collisions between cloud droplets, the formed droplets are moved to a new cloud droplet distribution if the "target classes" based on wet and dry sizes differ considerably. The number of bins reserved for these cloud droplets is between 20 and 30. After evaporation, particles from these bins are placed back to the original size distribution according to dry size. This decreases numerical diffusion and is important when cloud cycles are studied.

3. Results

3.1. Different coagulation kernels

Figure 1 shows how the different coagulation kernels affect the coagulation between particles of different sizes. The dissipation rate of turbulent energy is assumed to be 10 cm^2s^{-3}. In the atmosphere it typically varies between 3 cm^2s^{-3} and 2000 cm^2s^{-3} (Pruppacher and Klett, 1997) depending on the conditions. Typically, the values are low in cloud free conditions and high in strong cumulus convection. It can be seen from Fig. 1 that Brownian and Brownian diffusion enhancement are the only important coagulation mechanisms for small particles. In the early stages of a cloud, droplets coagulate due to Brownian enhancement and due to both turbulent mechanisms. If the

droplet distribution is narrow, the enhanced Brownian coagulation by the wake eddies and turbulent shear coagulation broaden the distribution and make also turbulent inertia efficient as a coagulation mechanism. Gravitational collection is important only for droplets larger than 10 μm in radius.

3.2. Coagulation scavenging

HNO_3 increases CDNC leading to a decrease in the mean size of the droplets. This also affects the coagulation scavenging of interstitial particles. The total cloud droplet surface area increases and so the Brownian coagulation rate increases. On the other hand, both gravitational and turbulence induced coagulation slow down. Figure 2 shows the effect of HNO_3 on the number of interstitial particles and cloud droplet number concentration. The aerosol particle size distribution (discretized into 200 size classes) is the continental distribution presented in Table 1, the updraft velocity is 1.0 m/s, the initial temperature is 285 K and the initial pressure is 900 mbar. Sulfuric acid production is not included in these simulations. With these values the water saturation ratio exceeds unity approximately 200 s into the simulation. Figure 2 also shows that the increased cloud droplet number concentration due to the uptake of HNO_3 enhances the coagulation scavenging. After 800 s, the total number of aerosol particles is approximately 50 cm^{-3} lower in the case of 4 ppb of HNO_3 present compared to the 0 ppb case. The reduction is mainly due to the decrease in the number concentration of particles with diameter around 20 nm (wet size in cloud). As can be seen from Fig. 3, particles smaller than 20 nm coagulate rapidly also when CDNC is smaller. The length of the simulation is chosen to be short enough to prevent effective droplet-droplet coalescence due to gravitational coagulation. In the 0 ppb case the decrease of CDNC due to coagulation is 6 cm^{-3}. In the 4 ppb case the decrease is 8.6 cm^{-3}, and so the relative decrease is not affected by HNO_3. From Figs. 3 e and f it can be seen that because of HNO_3, the mean size of the cloud droplets is clearly diminished and the number of maximas in the cloud droplet distribution formed through coagulation is smaller. This implies that rain formation can be delayed due to HNO_3.

However, in this case the distribution used contains big particles which are far from equilibrium (i.e. water saturation ratio on their surface stays clearly below unity) in the cloud and grow almost independently of CDNC and so the number of particles that reach the size of 50 µm in diameter at the end of the simulation is the same with and without HNO_3.

From the beginning of the simulation, the total aerosol number concentration decreases by approximately 850 cm^{-3}. 203 cm^{-3} of the decrease is due to adiabatic expansion of the air parcel, so the extra decrease due to HNO_3 is not negligible.

3.3. Sulfuric acid production

Sulfuric acid production increases the water soluble mass in cloud droplets. This affects both the direct and the indirect aerosol effect. Aerosol mass increases mainly in the accumulation mode, in which the particles are efficient scatterers and so the direct effect may be considerable in some situations (Yuskiewicz et al., 1999; Hegg et al., 1996). Changes in aerosol particle size distribution also affect the formation of cloud droplets during the next cloud cycle. Depending on the conditions, the number concentration of cloud droplets can either increase or decrease (Feingold and Kreidenweis, 2000).

From Table 2 we can see how HNO_3 affects the formation of sulfuric acid in the liquid phase when H_2O_2 and O_3 are compared as oxidants. In these simulations the updraft/downdraft velocity is 0.5 m/s, the initial temperature is 285.15 K and the continental aerosol distribution is from Table 1. The simulations are started at 90% relative humidity. The length of updraft/downdraft is 1000 s and the incloud residence time is around 1600 s during the cycle. After each cycle, the air parcel is kept at 90% *RH* for 1000 s to equilibrate the system kinetically. The oxidation capacity of O_3 is more pH dependent compared to H_2O_2 and so the condensation of HNO_3 decreases the amount of sulfuric acid produced. With H_2O_2 the sulfuric acid production does not decrease with increased HNO_3 concentration. Naturally, these results depend on the choice of simulation conditions, especially the acidicity of aerosol particle distribution,

the amount of ammonia and other gas phase species and the length of the simulation. For example with shorter cloud periods the difference in the amount of produced H_2SO_4 is even more clear and vice versa.

3.3.1. Implications for radiative effects

In Fig. 4, the effect of HNO_3 on aerosol size distributions after one cloud cycle is presented in the case of H_2O_2 induced H_2SO_4 production. Due to 1 ppb of HNO_3 98 cm^{-3} more cloud droplets form. The diameters of the smallest activated particles grow more than by a factor of 3 and the number concentration of particles larger than 200 nm in diameter increases. This can be remarkable, because the most efficient scatterers are particles with diameters between 200 nm and 800 nm (Yuskiewicz et al., 1999). To test this effect the total light-scattering is calculated according to Seinfeld and Pandis (1998) and the extinction coefficient according to Bohren and Huffman (1983). The refractive index was assumed constant at m=1.5–0.03i for all particles. In the case presented in Fig. 4, the total light-scattering increases from 3.1×10^{-5} m^{-1} (3.3×10^{-5} m^{-1} after initial equilibration with 1 ppb of HNO_3) to 1.01×10^{-4} m^{-1} when there is no HNO_3 in the gas and to 9.9×10^{-5} m^{-1} with 1 ppb of HNO_3. Hence the difference is not significant in this case. With other updraft velocities and/or aerosol distributions the highest sulfate production occurs in particles with different initial sizes. In Table 3 we have collected results with different updraft velocities and distributions (presented in Table 1). In the marine case it should be noted, that because of the large alkaline mode, 0.2 ppb of HNO_3 is not enough to increase the cloud droplet number concentration.

3.3.2. Implications for cloud droplet number concentration

Sulfuric acid production increases the bimodality of the aerosol size distribution. Particles will activate to cloud droplets more easily during the next cloud cycle because of increased mass. However, at the same time, increased mass will decrease the maximum supersaturation, and so the activation of particles not processed becomes more

unlikely. Therefore, if the updraft velocity is the same for every cycle, the number concentration of cloud droplets does not change. To study possible differences between the cases with and without HNO_3 and with and without sulfuric acid production a set of model simulations was done by varying the updraft velocities between the different cycles. For simplicity, coagulation is not included in these simulations.

We first consider a situation in which the updraft velocity is lower during the first cycle than during the following cycles. The first cycle produces H_2SO_4 to droplets that will activate in any case during the next cycles. This causes the maximum supersaturation to decrease during the following cycles, and the increased velocity does not increase the number concentration of activated particles as much as in the case without H_2SO_4-production. Results for the example cases are presented in Table 4. It is seen that if the velocity of the first cloud cycle is 0.1 m/s, CDNC is clearly decreased during the next cloud cycle. In the third cycle the velocity is increased to 1.0 m/s and the maximum saturation depression is not strong enough to decrease CDNC. In this simulation the height of the cloud is close to 100 m and thus almost all H_2O_2 is depleted during the first cycle.

If the updraft velocity of the first cycle is faster than that of the next cycles, the activation becomes easier. As can be seen from Table 4, especially in the case without HNO_3 the CDNC is clearly increased. On the third cycle, CDNC is even higher without HNO_3 than with 1 ppb of HNO_3. In this case the cloud height is close to 150 m and 150 ppt of H_2SO_4 is produced on the first cycle and 280 ppt during the second cycle.

4. Conclusions

In previous studies it has been shown that HNO_3 increases the number concentration of cloud droplets. In this study we take one step further and study how the increased droplet number concentration affects the cloud processing of the aerosol particle distribution. This is done with an air parcel model including condensation, coagulation and liquid phase chemistry. The coagulation kernel includes individual kernels for Brownian

coagulation, convective Brownian diffusion enhancement, gravitational collection, turbulent inertia, and turbulent shear. It was found that both Brownian coagulation mechanisms are important for interstitial aerosol particle scavenging and that turbulent shear and convective Brownian diffusion enhancement are the most important mechanisms for drop-drop collisions as long as cloud droplet distribution is narrow and gravitational collection is not efficient.

The increased cloud droplet number concentration due to HNO_3 was shown to speed up the scavenging of interstitial particles. The collision rate between cloud droplets in the early stages of cloud is lowered, but not substantially. Sulfuric acid production occurs in smaller particles, but the amount of acid produced decreases if ozone is the only oxidant available. However, when there is H_2O_2 in the system, the amount of sulfuric acid produced is independent of the HNO_3 concentration, and so the number of particles in accumulation mode increases more than without HNO_3. Due to HNO_3, the changes in the radiative properties of aerosol particles is smaller than without HNO_3. How the sulfuric acid production affects CDNC on the following cloud cycles, is dependent on the updraft velocity and initial aerosol particle distribution. In some cases it is even possible, that CDNC is smaller because of presence of HNO_3 during the previous cycle.

Acknowledgements. This study was supported by the Academy of Finland (project number 201052) and the Center-of-Excellence program.

References

Bohren, C. F. and Huffman, D. R.: Absorption and scattering of light by small particles, John Wiley & Sons inc., 1983. 10204

Bower, K. N. and Choularton, T. W.: Cloud processing of the cloud condensation nucleus spectrum and its climatological consequences, Q. J. R. Meteorol. Soc., 119, 655–679, 1993. 10198

Bromley, L. A.: Thermodynamic properties of strong electrolytes in aqueous solutions, AIChE J., 19, 313–320, 1973. 10200

Feingold, G. and Kreidenweis, S. M.: Does cloud processing of aerosol enhance droplet concentrations?, J. Geophys. Res., 105, 24 351–24 361, 2000. 10198, 10203

Hegg, D. A., Majeed, R., Yuen, P. F., Baker, M. B., and Larson, T. V.: The impacts of SO_2 oxidation in cloud drops and in haze particles on aerosol light scattering and CCN activity, Geophys. Res. Lett., 23, 2613–2616, 1996. 10203

Hegg, D. A.: Impact of gas-phase HNO_3 and NH_3 on microphysical processes in atmospheric clouds, Geophys. Res. Lett., 27, 2201–2204, 2000. 10199

Hegg, D. A., Covert, D. S., Jonsson, H., Khelif, D., and Friehe, C. A.: Observations of the impact of cloud processing on aerosol light-scattering efficiency, Tellus B, 56 (3), 285–293, 2004. 10198

Hoppel, W. A., Frick, G. M., Fitzgerald, J. W., and Larson, R. E.: Marine boundary layer measurements of new particle formation and the effects nonprecipitating clouds have on aerosol size distribution, J. Geophys. Res., 99, 14 443–14 459, 1994. 10198

Jacobson, M. Z.: Studying the effects of calcium and magnesium on size-distributed nitrate and ammonium with EQUISOLV II, Atmos. Environ., 33, 3635–3649, 1999. 10200

Jacobson, M. Z.: Fundamentals of atmospheric modeling, Cambridge University Press, Cambridge, 1999. 10201

Kokkola, H.: Model studies on the evolution of fogs and clouds in the presence of semi-volatile gases, PhD thesis, University of Kuopio, Department of applied physics, Report Series in Aerosol Science, 61, 2003. 10200

Kokkola, H., Romakkaniemi, S., and Laaksonen, A.: Köhler theory for polydisperse droplet populations in the presence of a soluble trace gas and an application to stratospheric STS droplet growth, Atmos. Chem. Phys., 3, 2139–2146, 2003, SRef-ID: 1680-7324/acp/2003-3-2139. 10200

Kulmala, M., Laaksonen, A., Korhonen, P., Vesala, T., Ahonen, T., and Barrett, J. C.: The effect of atmospheric nitric acid vapor on cloud condensation nucleus activation, J. Geophys. Res., 98, 22 949–22 958, 1993. 10199

Pruppacher, H. R. and Klett, J. D.: Microphysics of Clouds and Precipitation, Kluwer Academic Publishers, Netherlands, 1997. 10200, 10201

Roelofs, G.-J. and Jongen, S.: A model study of the influence of aerosol size and chemical properties on precipitation formation in warm clouds, J. Geophys. Res., 109,

doi:10.1029/2004JD004779, 2004. 10199
Romakkaniemi, S., Kokkola, H., and Laaksonen, A.: Parameterization of the nitric acid effect on CCN activation, Atmos. Chem. Phys., 5, 879–885, 2005, SRef-ID: 1680-7324/acp/2005-5-879. 10199
Saffman, P. G. and Turner, J. S.: On the collision of drops in turbulent clouds, J. Fluid Mech., 1, 16–30, 1956. 10201
Seinfeld, J. H. and Pandis, S. N.: Atmospheric Chemistry and Physics, From air pollution to climate change, Wiley, New York, 1998. 10198, 10204
Xue, H. and Feingold, G.: A modeling study of the effect of nitric acid on cloud properties, J. Geophys. Res., 109, doi:10.1029/2004JD004750, 2004. 10199
Yuskiewicz, B. A., Stratmann, F., Birmili, W., Wiedensohler, A., Swietlicki, E., Berg, O., and Zhou, J.: The effects of in-cloud mass production on atmospheric light scatter, Atmos. Res., 50, 265–288, 1999. 10198, 10203, 10204

Table 1. Trimodal distribution used in simulation. Particles are supposed to be internally mixed. In continental distribution 50% of mass is insoluble.

CONTINENTAL	mode 1	mode 2	mode 3
composition	$(NH_4)_2SO_4$/insoluble		
N[cm^{-3}]	1000	800	0.72
r_g[nm]	8.0	34	460
σ	1.60	2.16	2.20
MARINE	mode 1	mode 2	mode 3
composition	NH_4HSO_4		NaCl
N[cm^{-3}]	340	60	3.1
r_g[nm]	5.0	35	310
σ	1.60	2.00	2.70
RURAL	mode 1	mode 2	mode 3
composition		$(NH_4)_2SO_4$	
N[cm^{-3}]	10000	147	2000
r_g[nm]	7.5	27	342
σ	1.30	1.75	1.30

ACPD
5, 10197–10216, 2005

Table 2. Amount of sulfuric acid (unit ppt) produced in different conditions after 1, 2 and 5 cloud cycles.

C_{O3}=30 ppb, C_{SO2}=2 ppb	1	2	5
C_{HNO3}=1 ppt	82.2	117.5	178.4
C_{HNO3}= 100 ppt	57.1	88.2	144.9
C_{HNO3}=1 ppb	7.7	13.5	28.4
C_{H2O2}=0.5 ppb, C_{SO2}=2 ppb			
C_{HNO3}=1 ppt	410	481	500
C_{HNO3}=1 ppb	411	481	500

Table 3. The total light-scatter (unit $\times 10^{-5}$ m^{-1}) due to H_2SO_4 production. h is the height of cloud.

CONTINENTAL	h (m)	C_{HNO3}=1 ppt	C_{HNO3}=1 ppb
0.1 m/s	100	10.6	10.6
0.5 m/s	200	8.9	8.5
1.0 m/s	300	8.1	7.7
MARINE		C_{HNO3}=1 ppt	C_{HNO3}=0.2 ppb
1.0 m/s	300	14.3	14.4
RURAL		C_{HNO3}=1 ppt	C_{HNO3}=1 ppb
0.1 m/s	200	8.6	8.4
0.5 m/s	200	4.4	4.3
1.0 m/s	300	3.4	3.3

ACPD
5, 10197–10216, 2005

Table 4. Number of cloud droplets (cm^{-3}) during different cloud cycles. Values in parenthesis are without H_2SO_4-production.

C_{HNO3} \ velocity	0.1	0.2	1.0
0 ppb	118 (118)	133 (166)	337 (337)
1 ppb	149 (149)	184 (245)	436 (436)
C_{HNO3} \ velocity	1.0	0.2	0.1
0 ppb	337 (337)	337 (166)	267 (118)
1 ppb	436 (436)	387 (245)	245 (149)

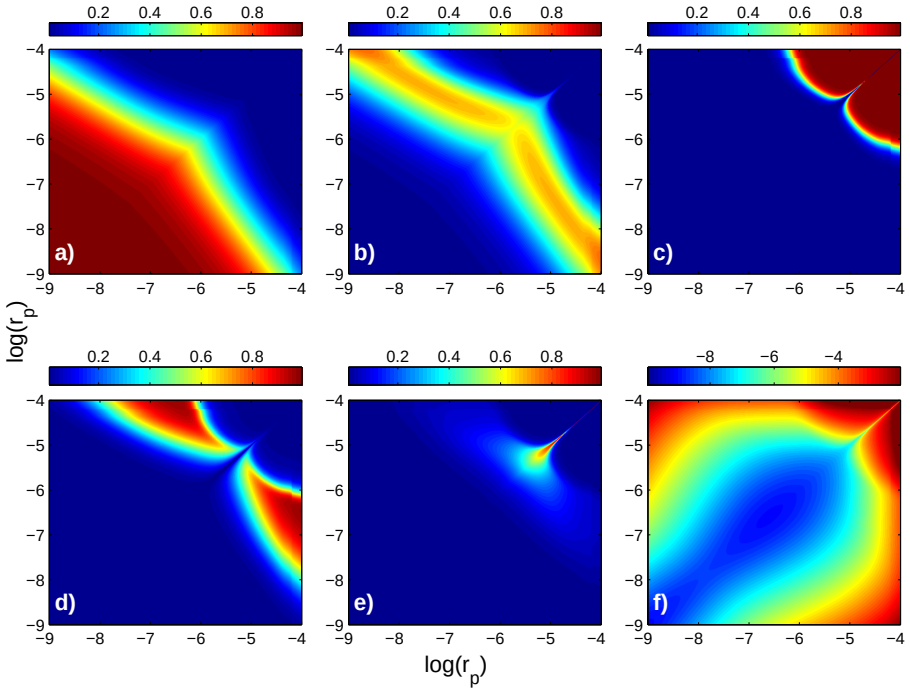

Fig. 1. Relative magnitude (K_i/K_{tot}, marked with color) of different coagulation kernels for different sized particles. Axes in figures are in logscale from 1 nm to 100 µm with the logarithm (10 base) of radius presented. Different kernels are **(a)** Brownian coagulation K_B, **(b)** convective Brownian diffusion enhancement K_{BE}, **(c)** gravitational collection K_G, **(d)** turbulent inertia K_{TI}, and **(e)** turbulent shear K_{TS}. In **(f)** the logarithm (10 base) of the total coagulation kernel (cm^3s^{-1}) is presented.

ACPD

5, 10197–10216, 2005

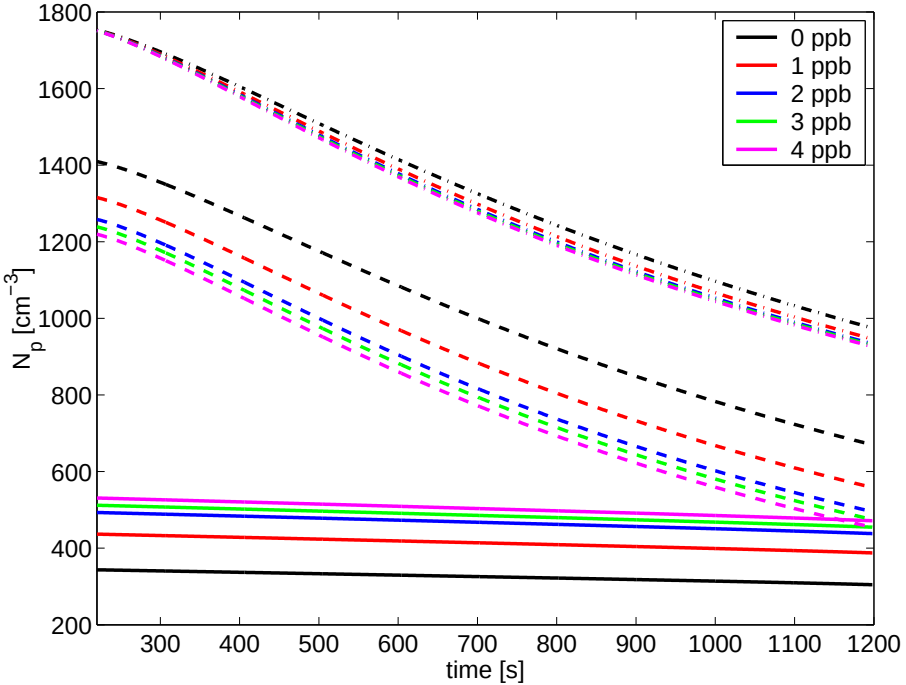

Fig. 2. Number of cloud droplets (solid lines) and interstitial particles (dashed lines), and the total number (dash-totted lines) as a function of time during the simulation for five different HNO_3 concentrations (different colors).

ACPD

5, 10197–10216, 2005

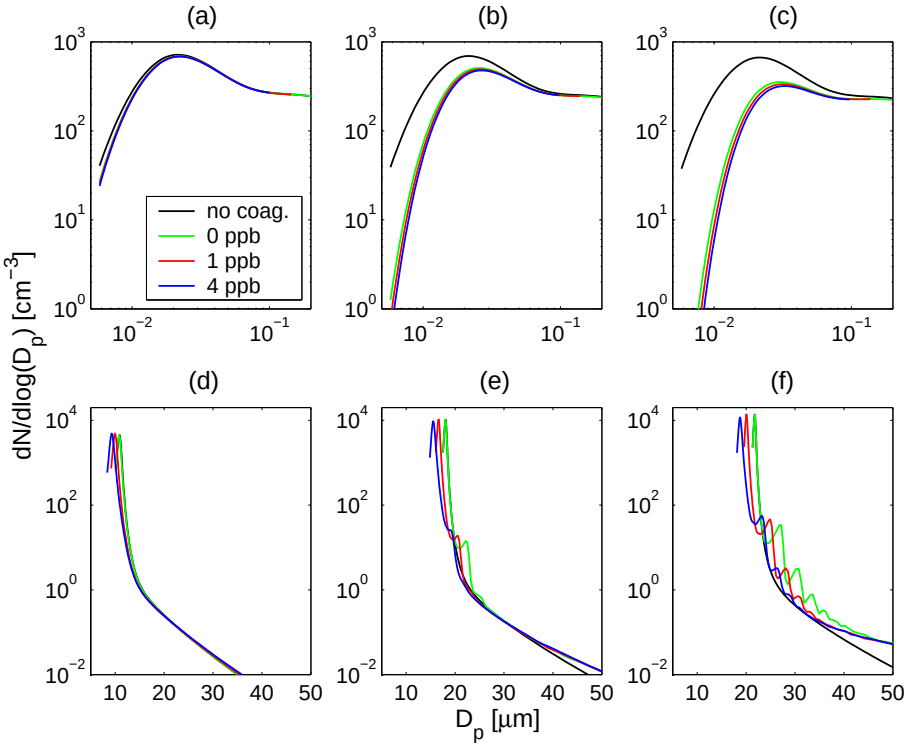

Fig. 3. Interstitial aerosol particles **(a, b, c)** and cloud droplets **(d, e, f)** 100 s (a, d), 500 s (b, e) and 900 s (c, f) after cloud formation. For reference, curves without coagulation (0 ppb of HNO_3) and with coagulation for 0 ppb, 1 ppb and 4 ppb of HNO_3 are presented.

ACPD
5, 10197–10216, 2005

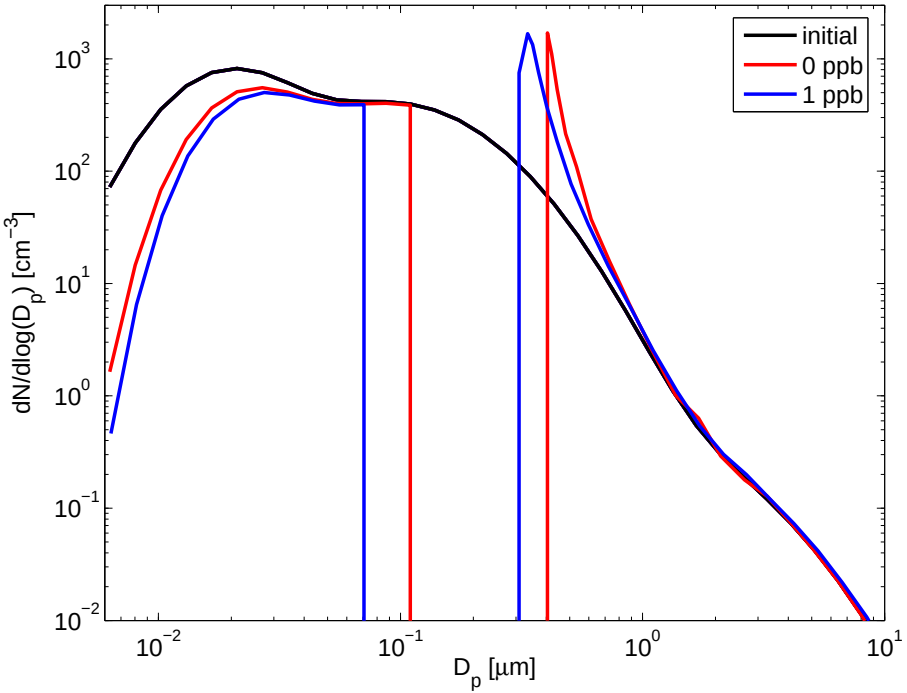

Fig. 4. Aerosol particle size distribution before and after one cloud cycle at *RH* of 90%, for two different HNO_3 concentrations.

ACPD
5, 10197–10216, 2005